Biochimica et Biophysica Acta 1788 (2009) 1138–1147

Contents lists available at ScienceDirect

Biochimica et Biophysica Acta

journal homepage: www.elsevier.com/locate/bbamem

Associated changes in HCN2 and HCN4 transcripts and I_f pacemaker current in myocytes

Qi Zhang, Aijie Huang, Yen-Chang Lin, Han-Gang Yu *

Center for Cardiovascular and Respiratory Sciences, Department of Physiology and Pharmacology, West Virginia University School of Medicine, Morgantown, West Virginia 26506, USA

ARTICLE INFO

Article history:
Received 23 October 2008
Received in revised form 7 February 2009
Accepted 11 February 2009
Available online 21 February 2009

Keywords:
Ratio of HCN transcript
HCN channel
Xenopus oocyte
shRNA
Pacemaker current
Rat ventricular myocytes

ABSTRACT

The time- and voltage-dependent inward current generated by the hyperpolarization-activated cyclic nucleotide-gated (HCN) channels contributes to the tissue-specific rhythmic activities in the brain and heart. Four isoforms (HCN1–HCN4) have been identified. Previous studies showed that different HCN isoforms may form functional heteromeric channels. We report here that when HCN2 and HCN4 mRNA were injected into *Xenopus* oocytes with various ratios of HCN2 over HCN4 at 1:1, 10:1, and 1:10, respectively, the resultant channels showed a depolarized current activation and significantly faster activation kinetics near the midpoint of activation compared with HCN4 homomeric channels. In adult rat myocytes overexpressing HCN4, there was an associated increase in HCN2 mRNA. In neonatal rat myocytes in which HCN2 was knocked down, there was also a simultaneous decrease in HCN4 mRNA. Coimmunoprecipitation experiments showed that HCN2 and HCN4 channel proteins can associate with each other in adult rat ventricles. Finally, in adult myocytes overexpressing HCN4, the hyperpolarization-activated inward current activation, I_f, was shifted to physiological voltages from non-physiological voltages, associated with faster activation kinetics. These data suggested that different ratios of HCN2 and HCN4 transcripts overlapping in different tissues also contribute to the tissue-specific properties of I_f.

1. Introduction

Hyperpolarization-activated current, I_h or I_f, contributes to many cellular functions such as resting membrane potential, synaptic transmission, and rhythmic activity in neurons and myocytes [1]. One of the unique features about this current is its distinct properties in different tissues [1]. The current is generated by the hyperpolarization-activated cyclic nucleotide-gated (HCN) pacemaker channels. Four isoforms (HCN1–4) have been identified [2–4]. Each isoform exhibits different gating properties when expressed in heterologous expressing systems such as *Xenopus* oocytes and HEK293 cells [2–4].

In many areas HCN channels are differentially expressed with overlap [1]. This raised a question for possible *in vivo* formation of HCN heteromeric channels. It has been reported that HCN1 and HCN2 can form a functional heteromeric channel in *Xenopus* oocytes [5,6] and mammalian cells (HEK293 and CHO cells) [7,8] as well as in neurons [5,6]. HCN1 and HCN4 were also shown to function as a heteromeric channel in sinoatrial node (SAN) cells [9]. Recently, HCN2 and HCN4 have been reported to co-assemble and form functional heteromeric channels in HEK293 and CHO cells, mouse embryonic heart, and rat thalamus [10,11].

In cardiac myocytes, I_f is the pacemaker current critical to the initiation and regulation of cardiac pacemaker activity [12]. Three HCN channel isoforms, HCN1, HCN2 and HCN4, are non-uniformly expressed in heart. All three are present in SAN cells with HCN4 being the prevalent form, whereas higher HCN2 and lower HCN4 have been detected in ventricles [13]. Interestingly, the ratio of HCN2 over HCN4 transcript changes from 5:1 in the neonate to 13:1 in the adult, which is accompanied with a hyperpolarizing shift of I_f activation [13]. It remains an open question whether the ratio of HCN2 and HCN4 transcripts is a contributing factor to changes in the biophysical properties of I_f in ventricular myocytes. Moreover, it has not been reported whether HCN2 and HCN4 channel proteins can associate with each other in cardiac ventricular myocytes. The present work was designed to address these questions.

2. Methods

2.1. Heterologous expression of HCN2 and HCN4 in Xenopus oocytes

Oocytes were prepared from stage V mature female *Xenopus laevis* as previously described [14]. Oocytes were injected with 50 nl of cRNA (0.1 ng/nl) made from mouse HCN2 and human HCN4 cDNA plasmids. Injected oocytes were incubated at 18 °C for 24–96 h prior to voltage clamp recordings. For electrophysiological studies, oocytes were voltage-clamped using a two-microelectrode voltage clamp setup. The holding potential was −30 mV. The extracellular recording solution contained (mM): 80 NaCl, 2 KCl, 1 $MgCl_2$, and 5 Na-HEPES (pH 7.6). The threshold activation of current was defined as the least

* Corresponding author. Tel.: +304 293 2324; fax: +304 293 5513.
E-mail address: hyu@hsc.wvu.edu (H.-G. Yu).

0005-2736/$ – see front matter © 2009 Elsevier B.V. All rights reserved.
doi:10.1016/j.bbamem.2009.02.011

negative voltage at which the current could be readily measured over the noise with amplitude no less than 10–20 pA.

2.2. Heterologous expression of HCN2 and HCN4 in HEK293 cells

Mouse HCN2 cDNA in oocyte expression vector, pGH, was initially obtained from Drs. Bina Santoro/Steve Siegelbaum (Columbia University). We subcloned it into the EcoRI/XbaI sites of pcDNA3.1 mammalian expression vector (Invitrogen) for functional expression in mammalian cells. Human HCN4 cDNA was originally provided as a gift by Dr. U.B. Kaupp (Institut für Biologische Informationsverarbeitung, Germany). We subcloned it into the HindIII/Xba sites of pcDNA3.1.

HEK293 cells were grown in Dulbecco's modified Eagle's medium (DMEM, Invitrogen), supplemented with 10% fetal bovine serum, 100 IU/ml penicillin, and 100 g/l streptomycin. Cells with 50–70% confluence in 6-well plate were used for HCN2 and HCN4 plasmids transfection using Lipofectamine2000 (Invitrogen). HCN was co-transfected with GFP for easy selection of cells for patch clamp studies.

2.3. Whole-cell patch clamp recordings of HCN in HEK cells and in I_f in myocytes

After 24–96 h transfection cells with green fluorescence were selected for patch clamp experiments. The HEK293 cells were placed in a Lucite bath in which the temperature was maintained at 25 °C ± 1 °C by a temperature controller (Cell MicroControls, VA). I_f/I_{HCN} currents were recorded using the whole-cell patch clamp technique with an Axopatch-200B amplifier. The pipettes had a resistance of 2–4 MΩ when filled with internal solution (mM: NaCl 6, K-aspartate 130, $MgCl_2$ 2, $CaCl_2$ 5, EGTA 11, and HEPES 10; pH adjusted to 7.2 by KOH). The external solution contains (mM) NaCl 120, $MgCl_2$ 1, HEPES 5, KCl 30, $CaCl_2$ 1.8, and pH was adjusted to 7.4 by NaOH. The I_{to} blocker, 4-AP (2 mM), was added to the external solution to inhibit the endogenous transient potassium current, which can overlap with and obscure I_{HCN} tail currents recorded at +20 mV. Data were acquired by CLAMPEX and analyzed by CLAMPFIT (pClamp 8, Axon).

Due to slow activation kinetics of HCN4, currents elicited by hyperpolarizing pulses near the threshold activation of the channel (e.g., −85 mV to −105 mV) did not reach steady states even in response to the 20-second pulses. We thus fit the current traces to the steady states with an exponential function. We then divided the amplitude of the steady state current trace by that measured from 20-second current amplitude and obtained a ratio (always greater than 1). We then multiplied this ratio to the corresponding tail currents which were then used to construct the activation curves.

The freshly isolated myocytes were placed in a Lucite bath in which the temperature was maintained at 35 °C ± 1 °C by a temperature controller (Cell MicroControls, VA). I_f currents were recorded using the whole-cell patch clamp technique with an Axopatch-700B amplifier (Axon). The external solution contained (mM) NaCl 140, KCl 5.4, $CaCl_2$ 1.8, $MgCl_2$ 1, and Glucose 10, $NiCl_2$ 0.1, $BaCl_2$, 5, 4-AP 2, TTX 0.03, pH 7.4. The pipettes had a resistance of 2–4 MΩ when filled with internal solution composed of (mM) NaCl 6, K-aspartate 130, $MgCl_2$ 2, $CaCl_2$ 1, Na_2-ATP 2, Na-GTP 0.1, HEPES 10, pH 7.2. Sodium (I_{Na}) and potassium (I_{to}) current blockers, tetrodotoxin (TTX) and 4-aminopyridine (4-AP), were added to the external solution to inhibit the sodium and transient potassium currents. During I_f recording, $BaCl_2$ was added to the external solution to block I_{K1} background potassium current which can mask I_f current.

Data are shown as mean ± SEM. The threshold activation of I_f is defined as the first hyperpolarizing voltage at which the time-dependent inward current can be observed. Student's *t*-test and one-way ANOVA were used for statistical analysis. $p<0.05$ was considered as statistically significant.

The patch clamp setup is also equipped with bright-field and fluorescent light sources. It also has CCD camera attached to take either bright-field or fluorescent image of the same batch of myocytes.

2.4. Cardiac tissue and myocyte preparation

Adult (300–350 g, about 3 month old) and neonatal (days 1–3) rats were euthanized by intraperitoneal injection of pentobarbitol in accordance with the Institutional Animal Care and Use Committee protocols. The heart was excised and ventricles were cut out and prepared for protein chemistry experiments, as previously reported [15].

The adult rat ventricular myocytes were prepared using a collagenase dissociation protocol as previously described [15,16]. Briefly, the aorta was cannulated and the heart was retrogradely perfused with oxygenated Ca^{2+}-free Tyrode solution at 37 °C for 5 min, followed by oxygenated Ca^{2+}-free Tyrode solution containing 0.6 mg/ml collagenase II (Worthington Biochemical) for 20–30 min. The ventricles were minced into small pieces in KB solution, dispersed, and filtrated through a 200 μm mesh.

The neonatal rat ventricular myocytes were prepared using a modified method as previously described [17]. Briefly, whole hearts were minced in Ca^{2+}- and Mg^{2+}-free D-Hanks solution (mM): KH_2PO_4 0.06, NaCl 8.0, $NaHCO_3$ 0.35, KCl 0.4, Na_2HPO_4 0.05. The myocardial cells were dispersed by the addition of Hanks solution containing trypsin 0.1% and then were stirred at 37 °C. The supernatant was removed and discarded. Cells were incubated with fresh trypsin 0.1% for 20 min at 37 °C. The supernatant was collected, and cells were isolated by centrifugation in a tabletop centrifuge for 5 min at 1000 rpm at room temperature. Cells were resuspended in 5 ml DMEM supplemented with 10% fetal bovine serum and kept at 37 °C. The digestion step was repeated four times, and cell suspensions from each digestion were combined and centrifuged at 1000 rpm for 5 min. Cells were then resuspended in DMEM (1.8 mM Ca^{2+}) supplemented with 10% horse serum, 5% FCS, 0.1 mmol/l 5-bromo-deoxyuridine and 1% antibiotics (10,000 U/ml penicillin and 10,000 μg/ml streptomycin). The myocyte-enriched suspension was transferred to culture dishes at a density of approximately 1.5×10^6 cells per 60-mm culture dish.

2.5. Co-immunoprecipitation

Total protein extracts were prepared from heart tissues using CytoBuster Protein Extraction Reagent (Novagen). The protein concentration of the lysate was determined using the Bradford method. Equal amounts of total protein (1.0 g) were incubated with a specific antibody for 1 h at 4 °C, and protein A/G PLUS-agarose (Santa Cruz) was then added and incubated overnight with gentle rock. The beads were washed extensively with cold PBS buffer, and resuspended in 2× Laemmli sample buffer. The immune complexes were separated by SDS-PAGE and analyzed by Western blot using an anti-HCN4 or an anti-HCN2 polyclonal antibody (Alomone).

2.6. Viral transduction of cardiac myocytes

2.6.1. Cell culture for adult and neonatal rat ventricular myocytes

Freshly isolated adult rat myocytes were suspended in culture media M199 supplemented with 0.2% albumin, 5 mM taurine, 3.0 mM creatine, 3.0 mM carnitine, 0.1 μM insulin and 1% antibiotics (100 IU/ml penicillin, 50 IU/ml streptomycin, Sigma). After counting the cells using a hemocytometer, approximately 3×10^5 cells were plated in each well of the 6-well plates that were pre-coated with laminin (Sigma) 24 h prior to the myocyte isolation and kept in cell culture incubator at 37 °C. The cells were allowed to attach for 1 h and then the media was changed with fresh culture media to remove unattached myocytes. The isolated cells were further cultured for 1 h before infection.

Freshly isolated neonatal myocytes were preplated to reduce fibroblast proliferation, cultured initially in serum-containing medium, and then switched to serum-free medium after 24 h. Most fibroblast cells were removed by collecting neonatal myocytes in the supernatant within 1–2 h after isolation. Myocytes were cultured in DMEM-Medium199 (4:1) supplemented with 5% FBS, 5% horse serum, 1% L-glutamine and 1% penicillin/streptomycin. Myocytes were treated with mitomycin C (0.1–1 μM) to prevent further fibroblast cell growth. Final cell populations contained more than 95% growth-arrested cardiomyocytes, as assessed by immunofluorescence analysis.

For infection, the lentivirus stock was applied at MOI (multiplicity of infection) = 10 in the presence of 8 μg/ml polybrene (Sigma). Empty lentivirus was used in parallel to infect myocytes as a negative control. All subsequent experiments were carried out at 48–72 h after infection. The infection efficacy was higher in neonatal (>95%) than in adult ventricular myocytes (>80%).

2.6.2. Design of HCN2-shRNA and subcloning HCN2-shRNA and HCN4 into lentiviral vectors

For small-hairpin RNA design for HCN, three shRNA nucleotides (1. TCCAGGAGATTGTCAAATGTGACTGT, 2. CGTGGTTTCGGATACTTTCTTCCTCA, 3. CGCACCGGCATTGTTATTGAGGACAA) against the rat/mouse HCN2 gene (designed by using Invitrogen online shRNA designing tool) were inserted into BamHI/EcoRI site of lentivirus vector pSIF1-H1-copGFP (SBI, Mountain View, CA). These three constructs were designated as HCN2-shRNA-1, HCN2-shRNA-2, and HCN2-shRNA-3. HCN2-shRNA-2 achieved the inhibitory effect of >90%. HCN2-shRNA-1 achieved inhibitory effect of about 80%). HCN2-shRNA-3 did not have significant inhibitory effect. We used HCN2-shRNA-2 throughout the following experiments in myocytes, and used name HCN2-shRNA. The shRNA constructs were co-transfected with recombinant plasmid pcDNA3.1/myc-His containing mHCN2 gene to screen their efficacy in HEK293 cells. As a negative control, pSIF1-H1-siLuc-copGFP (target luciferase) was co-transfected with the target recombinant plasmids. After 48–72 h incubation, cells were harvested and total protein extracts were prepared. Real time RT-PCR and Western blot analysis were carried out to select the effective construct. The functional efficacy of HCN2-shRNA was further tested and confirmed using whole-cell patch clamp in HEK293 cells expressing HCN2 channels.

Full-length of human HCN4 cDNA was subcloned into Xba I site of pCDF1-MCS2-EF1-copGFP™ (SBI) to generate plasmid pCDF1-hHCN4. Correct insert in the desired orientation was verified by restriction digest and DNA sequencing.

2.6.3. Lentivirus production

HEK293TN (SBI) cells were seeded in 10-cm plate the day before transfection. When cells reached 50–70% confluence, cells were co-transfected with 10 μg of the Packaging Plasmid Mix (SBI) and 2 μg HCN2-shRNA or hHCN4 using Lipofectamine™/Plus™ Reagent (Invitrogen). Supernatants at 48–72 h post transfection were collected and centrifuged at 3000 rpm for 5 min to pellet cell debris and filtered the supernatant through Millex-HV 0.45 μm PVDF filters (Millipore). Lentiviral pseudovirus was concentrated using PEG-it™ Virus Precipitation Solution (5X, SBI) and stored at −80 °C. Titer estimation of lentivirus was subsequently carried out by Fluorescence-activated cell-sorting (FACS) analysis.

2.7. Test of HCN2-shRNA in HEK293 cells

To test the specificity of shRNA-HCN2, HEK293 cells with 90–95% confluence in 96-well plate were co-transfected with pcDNA3.1-HCN4 and shRNA-HCN2 (SBI). As a negative control, empty vector pSIF1-H1-copGFP was also co-transfected with pcDNA3.1-HCN4 at the same time. 18–24 h after transfection, total RNA was extracted and transcribed reversely into cDNA using Cells-to-cDNA II kit (Ambion).

2.8. Real-time RT-PCR

Total RNA was isolated from same amount (~10^5) and same incubation time (48–72 h) of infected myocyte cells using RNAqueous-4PCR kit (Ambion) and transcribed reversely into cDNA with High Capacity cDNA Reverse Transcription Kit. Relative quantification of HCN2 and HCN4 mRNA was performed on 1.5 μl of each cDNA preparation using Universal TaqMan Master Mix (Applied Biosystems) and TaqMan® Gene Expression Assays (Applied Biosystems, Assay ID: Rn01408575_gH for HCN2, Assay ID: Hs00175760_m1 and Rn00572232_m1 for HCN4) in an ABI HT7900 Sequence Detection System. The TaqMan Assay targeting 18S rRNA (Applied Biosystems, Assay ID: Hs99999901_s1) was used as an endogenous control to normalize differences in RNA input. After confirmation that the amplification efficiency of HCN genes and the endogenous control 18S rRNA were approximately equal, differences were calculated with the threshold cycle (Ct), and the comparative Ct method was used for relative quantification [18].

3. Results

3.1. Functional expression of HCN2 and HCN4 in Xenopus oocytes and in HEK cells

We first tested the idea that oocytes injected with mixed HCN2 and HCN4 mRNA might express resultant channels with gating properties different from HCN2 or HCN4 homomeric channels if HCN2 and HCN4 indeed form heteromeric channels.

Fig. 1 shows the currents recorded from oocytes 48 h after injection. Ratio of HCN2 over HCN4 mRNA used for injection was 1:10 (A), 1:1 (B), and 10:1 (C), respectively. HCN2 (D) and HCN4 (E) mRNA were also injected separately to serve as controls. Hyperpolarizing pulses from −55 mV to −115 mV in 10 mV increment for 8 s were applied (A–C). Hyperpolarizing pulses from −65 mV to −115 mV and −75 mV to −135 mV for 7 s were used for HCN2 and HCN4, respectively. To analyze the gating properties, we constructed the activation curve by dividing the tail currents recorded at +10 mV (Etest) by the driving force (Etest-Erev, the reversal potential in each oocyte was measured). For slow activation of HCN2 and HCN4 around the midpoint of current activation (whether individually expressed or coexpressed), we applied longer pulses (an illustration is provided in Fig. 1F) to obtain the current traces that allow us to perform Boltzmann best fit with single exponential function.

Fig. 2 shows the voltage-dependent activation kinetics (A–E) and the midpoint activations ($V_{1/2}$) (F). In comparison to HCN2 (1:0) or HCN4 (0:1) homomeric channels, mixed HCN2/HCN4 channels all exhibited a depolarizing shift in voltage-dependent activation. Averaged $V_{1/2}$ of HCN2/HCN4 was -94 ± 2 mV, -104 ± 2 mV, -82 ± 3 mV, -86 ± 2 mV, -84 ± 3 mV for ratios of 1:0, 0:1, 1:10, 1:1, and 10:1, respectively. The slope factors were not significantly altered (7.4 ± 0.6, 8.8 ± 0.8, 8.4 ± 0.5, 7.8 ± 0.6, 7.5 ± 0.9, for 1:0, 0:1, 1:10, 1:1, and 10:1, respectively).

The voltage-dependent activation of HCN2 and HCN4 has been studied in HEK293 cells and different values for midpoint activation of HCN2 and HCN4 have been reported [19–23]. Fig. 3 shows the current expression of HCN2 (A) and HCN4 (B) subcloned in pcDNA3 (a widely used vector for exogenous protein expression in mammalian context) under our experimental conditions. The midpoint activation were -83 ± 4 mV ($n = 5$) for HCN2 and -90 ± 3 mV ($n = 5$) for HCN4. Since we focused on the potential contribution of relative mRNA ratio of HCN2 over HCN4 to the voltage-dependent activation of the heteromeric channels, we will not consider the post-translational modulation of HCN channels (e.g., protein

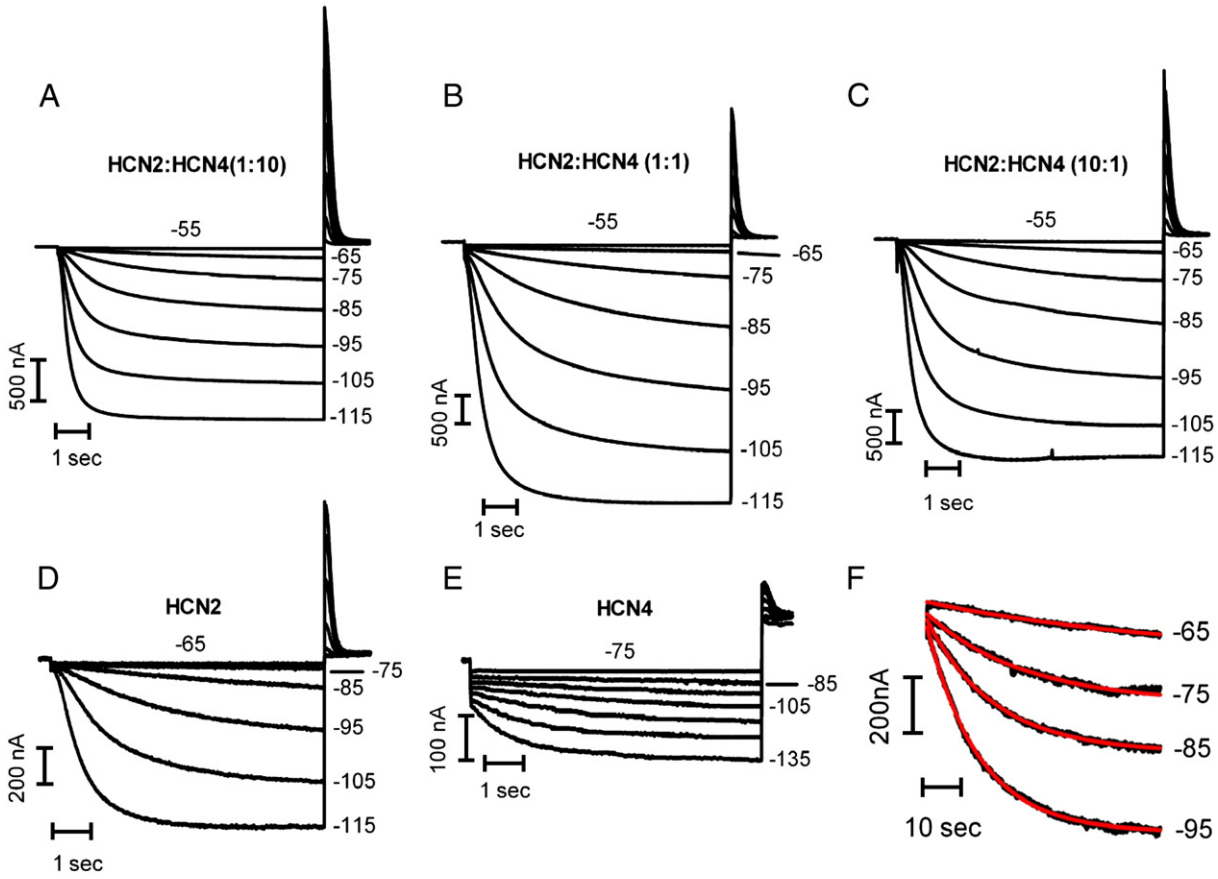

Fig. 1. Functional co-expression of HCN2 and HCN4 in *Xenopus* oocytes. HCN2 and HCN4 mRNA at the ratio of 1:10 (A), 1:1 (B), and 10:1 (C) were injected into oocytes. The resultant channel currents were elicited by 8-second hyperpolarizing pulses ranging from −55 mV to −115 mV in 10 mV increment and stepped back to 10 mV for recording tail currents. (D) Expression of HCN2 alone in oocytes. The current trace at −55 mV was not shown due to no activation until −75 mV. (E) Expression of HCN4 alone in oocytes. The more hyperpolarized pulses (−75 mV to −135 mV in 10 mV increments) were used to reflect the more negative activation of HCN4. The holding potential was −30 mV. One current trace without activation was kept in panels A–D to emphasize the threshold activation at the next voltage. (F) Illustration of Boltzmann best fit with one exponential function on slow HCN currents (dark lines) activated by 60 second hyperpolarizing pulses from −65 mV to −95 mV to allow full current activation. The red lines were the fit curves after initial delay in current activation.

glycosylation [10] and phosphorylation [24–26] as well as lipid-mediated kinases [27,28]) that can dramatically affect the gating of HCN2 and HCN4 expressed in HEK293 cells.

The voltage-dependent current activation kinetics showed that HCN2/HCN4 at all ratios activated significantly faster than HCN4 homomeric channels (Fig. 2E), but not HCN2 channels (Fig. 2D). The voltages at which the slowest activation occurred were shifted to depolarized potentials, consistent with the positive shift in midpoint activation ($n=7$–12). These data suggested that mixture of HCN2 and HCN4 mRNA can produce the resultant functional channels with gating properties different from their homomeric channels, which favors the hypothesis for the possible formation of functional heteromeric channels.

Given that the transcript levels for HCN2 and HCN4 are different in ventricles and change during development [29], we decided to examine the mRNA levels of one isoform when that of the other is altered.

3.2. Linked decrease in HCN4 mRNA with inhibited HCN2 mRNA in neonatal rat myocytes

Due to relatively higher HCN2 and HCN4 transcripts in neonatal than in adult rat ventricles, we first tested the hypothesis that inhibiting mRNA levels of one isoform may alter that of the other. We designed several small hairpin RNA (shRNA) nucleotides that specifically targeted a mouse HCN2 gene, inserted them into a shRNA-expressing lentiviral vector. We screened these nucleotides for their efficacy in knocking down HCN2 expression at levels of mRNA and protein and ionic currents by co-transfecting them respectively with a target gene into HEK293 cells [30].

Fig. 4 shows a typical set of experiments performed to test the efficacy of inhibition of HCN2 channel activity in HEK293 cells. First, we examined the changes in HCN2 mRNA (normalized to 18S) by HCN2-shRNA using RT-PCR (Fig. 4A). The left panel shows $85.0\pm1.5\%$ ($n=5$, $p<0.05$) inhibition of HCN2 mRNA. The empty vector was used as a control. Second, we performed Western blotting analysis to confirm that a significant reduction of HCN2 channel protein was accompanied with its mRNA decrease. Indeed, Fig. 4B shows that HCN2-shRNA inhibited the HCN2 signal in comparison to the cells transfected HCN2 alone or the empty vector. HCN4 transfected or non-transfected (NT) HEK293 cells were used as a specificity control for HCN2 antibody and a negative control, respectively. The averaged inhibition was $84.0\pm1.4\%$ ($n=5$, $p<0.05$) (right panel of Fig. 4A). Inhibited HCN2 at both mRNA and protein levels indicated a classical RNAi mechanism by HCN2-shRNA. Finally, we tested functional efficacy of HCN2-shRNA inhibition by recording the HCN2 current in HEK293 cells expressing HCN2 channels. The functional current expression of HCN2 was not affected by empty vector transfection (Fig. 4C), but nearly blocked by co-transfecting HEK293 cells with HCN2-shRNA (Fig. 4D). The mean I_{HCN2} measured at −95 mV was reduced by $96\pm1\%$, $n=5$, $p<0.05$ (Fig. 4E).

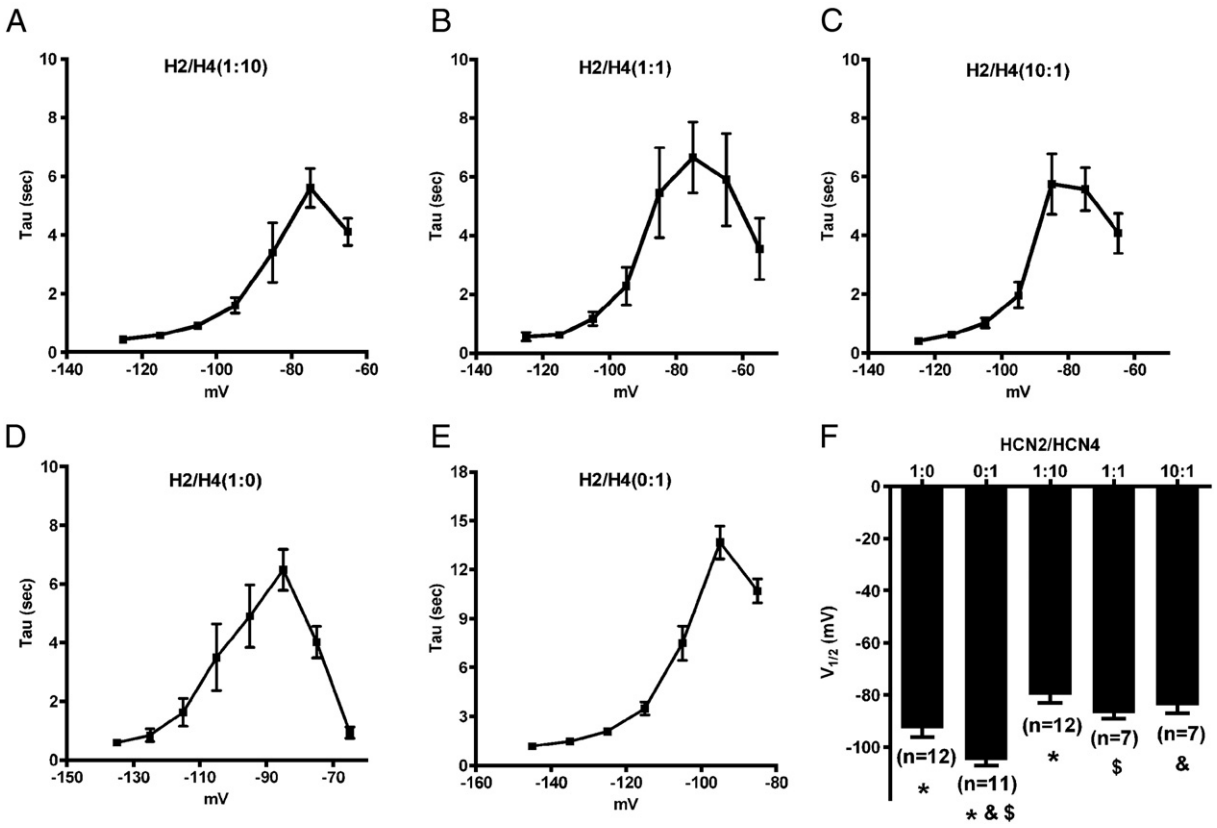

Fig. 2. Gating properties of co-expressed HCN2/4 channels. Voltage dependent activation kinetics for HCN2/HCN4 channels at ratios of 1:10 (A), 1:1 (B), 10:1 (C), 1:0 (D), and 0:1 (E), respectively. (F) Averaged midpoint activation of mixed HCN2 and HCN4 channels as compared to HCN2 and HCN4 homomeric channels. Symbols *, &, and $ indicated statistical significance for the corresponding pairs ($p<0.05$).

We then introduced the most effective HCN2-shRNA into neonatal rat ventricular myocytes (NRVM) mediated by lentivirus. Fig. 5A shows images before (brightfield) and after (fluorescence) lentiviral infection of the same neonatal rat ventricular myocytes, indicating that most, if not all, myocytes can be effectively infected by lentivirus which is tagged by GFP. Fig. 5B shows that the HCN2 mRNA level was inhibited by $88\pm3\%$ ($n=5$, $p<0.05$) with HCN2-shRNA. Infection of empty viral vector tagged with GFP itself had little effect on HCN2 mRNA levels. However, there was an associated down-regulation of HCN4 mRNA ($62\pm6\%$, $n=5$, $p<0.05$), which is in comparison to the control experiment that the infection of empty viral vector tagged with GFP had little effect on HCN4 mRNA levels (Fig. 5C). To exclude the potential off-target effect of HCN2-shRNA nucleotides on HCN4 mRNA, we examined the potential inhibition of HCN2-shRNA on HCN4, an isoform in the same family. In cells overexpressing HCN4, little effect ($92\pm8\%$, $n=3$, $p>0.05$) of HCN2-shRNA on HCN4 mRNA was observed as compared to the control (GFP-tagged empty vector infection) (Fig. 5D). The protein expression level of HCN4 was not affected, either (Fig. 5E). Western blot experiment was repeated at least three times.

3.3. Linked increase in HCN2 mRNA with increased HCN4 mRNA in adult rat ventricular myocytes

We next tested the idea that increasing mRNA of one isoform may increase mRNA of the other. We subcloned a human HCN4 gene into the lentiviral vector and infected adult rat myocytes (see Methods for details). Fig. 6A shows the images before (bright-field) and after (fluorescence) lentiviral infection in the same myocyte. RT-PCR results show that the levels of the endogenous rat HCN4 (rHCN4) mRNA were increased by 2.8 ± 0.7 fold ($n=5$, $p<0.05$)) (Fig. 6B). Interestingly again, the endogenous rat HCN2 (rHCN2) mRNA levels were also up-regulated by 4.3 ± 0.8 fold ($n=5$, $p<0.05$) (Fig. 6C).

3.4. Association of HCN2 and HCN4 channel proteins in adult rat ventricular myocytes

In combination of the functional expression studies of mixed HCN2 and HCN4 channels that favored the formation of heteromeric channels in oocytes and associated change in transcript of one isoform while the mRNA level of the other is changed in myocytes, it is likely that the HCN2 and HCN4 channel proteins are associated in adult rat ventricular myocytes.

Fig. 7 shows that the ventricular sample was first immunoprecipitated using a specific anti-HCN4 antibody, and the HCN2 signal was then detected using a specific anti-HCN2 antibody (Fig. 7A). There are two HCN2 bands (one near 100 kDa and the other near 112 kDa) representing the glycosylated (mature) and unglycosylated forms [10]. If the sample was first immunoprecipitated using a specific HCN2 antibody, the HCN4 signals were readily detected with an HCN4 antibody (Fig. 7B). Samples immunoprecipitated using the same antibody and non-transfected HEK293 cells (marked Control) were used as a positive control and a negative control, respectively. The specificities of HCN2 and HCN4 antibodies have been previously tested [15,24,31]. The results supported the notion that HCN2 and HCN4 proteins can associate with each other in adult rat ventricles.

3.5. I_f in adult rat ventricular myocytes overexpressing HCN4

If the ratio of HCN2 over HCN4 transcript is also a contributing factor to the voltage-dependent activation of I_f, an altered ratio of HCN2 over HCN4 should change I_f. We have previously shown that the

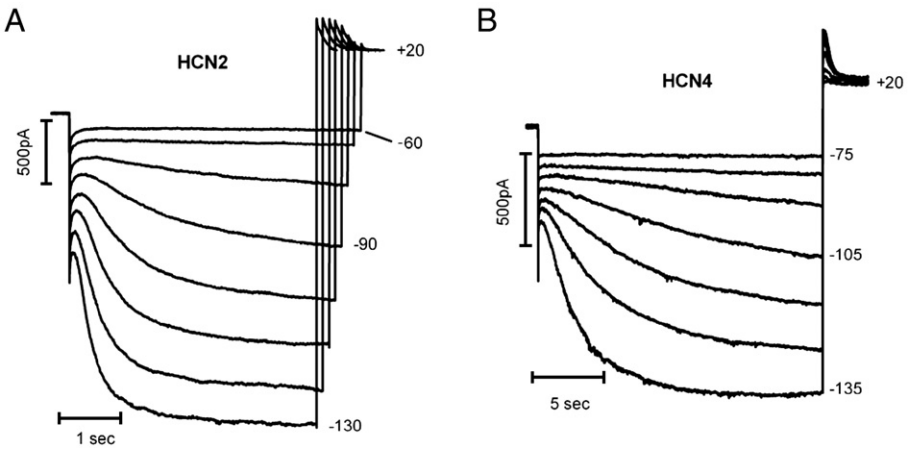

Fig. 3. Expression of HCN2 and HCN4 in HEK cells. (A) HCN2 currents were elicited by hyperpolarizing pulses with variable durations from −55 mV to −125 mV in 10 mV increments. (B) HCN4 currents were elicited by 20 s hyperpolarizing pulses from −75 mV to −135 mV in 10 mV increments. The holding potential was −10 mV. Tail currents were recorded at +20 mV.

ratio of HCN2 over HCN4 increases more than 2-fold from neonate to adult, accompanied with a hyperpolarized shift of I_f activation [13]. If we increase the ratio by increasing HCN4 in adult rat ventricles, which will decrease the HCN2/HCN4 ratio, we would expect to observe a depolarized shift of I_f activation.

Fig. 8 provided a typical set of protein biochemistry and electrophysiological data showing an increased expression of HCN4 and an altered I_f after we over-expressed HCN4 mediated by lentivirus (see Methods for details). Fig. 8D showed that HCN4 proteins were barely detected (non-infected lane) by Western blot analysis due to its low expression in adult rat ventricle [13]. But the signals can be readily detected for myocytes overexpressing HCN4 (in three samples). The associated increase in I_f current expression was shown in Fig. 8B. The currents were elicited by 4.5-second hyperpolarizing pulses from −70 mV to −140 mV (Fig. 8A, C) or variable pulse durations (Fig. 8B) in 10 mV increments. The tail currents were recorded at +20 mV. To verify the enhanced time-dependent inward current was indeed I_f, we applied 4 mM Cs to block it shown in the inset of Fig. 8B. The current density measured at −120 mV or −125 mV was 5.6 ± 1.9 pA/pF (n = 8) for HCN4-infected myocytes, 0.9 ± 1.1 pA/pF (n = 10) for non-infected myocytes (Fig. 8A), and 0.7 ± 0.8 pA/pF (n = 5) for vector-infected myocytes (Fig. 8C). The increased I_f current density is statistically significant in comparison to either non-infected or vector-infected myocytes (p<0.05). There is no statistical difference

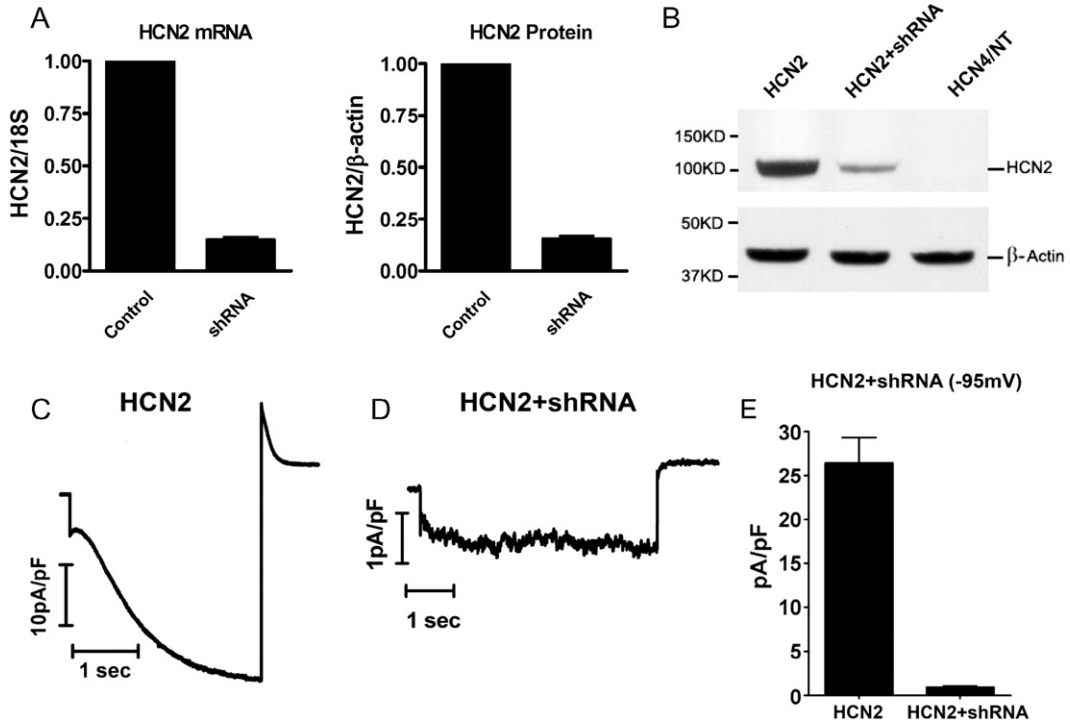

Fig. 4. shRNA inhibition of HCN2 channels in HEK293 cells. (A) Quantitative shRNA inhibition of HCN2 mRNA (left panel) and protein (right panel). RNA Quantification was calculated by normalization of mRNA to 18S. Protein quantification was carried out by normalization of protein to β-actin. (B) Immunoblots of HCN2 signal detection by an anti-HCN2 antibody in cells co-transfected with HCN2 and the empty vector, with HCN2 and HCN2-shRNA, and with either HCN4 only or non-transfection, respectively. (C) HEK293 cells were transfected by HCN2 and empty vector. HCN2 current was activated by a 3-second hyperpolarizing pulse to −95 mV from a holding potential of −10 mV. (D) HEK293 cells were affected by HCN2 and HCN2-shRNA. HCN2 current was activated by a 3-second hyperpolarizing pulse to −95 mV from a holding potential of −10 mV. (E) Mean current density of HCN2 in the control and HCN2-shRNA.

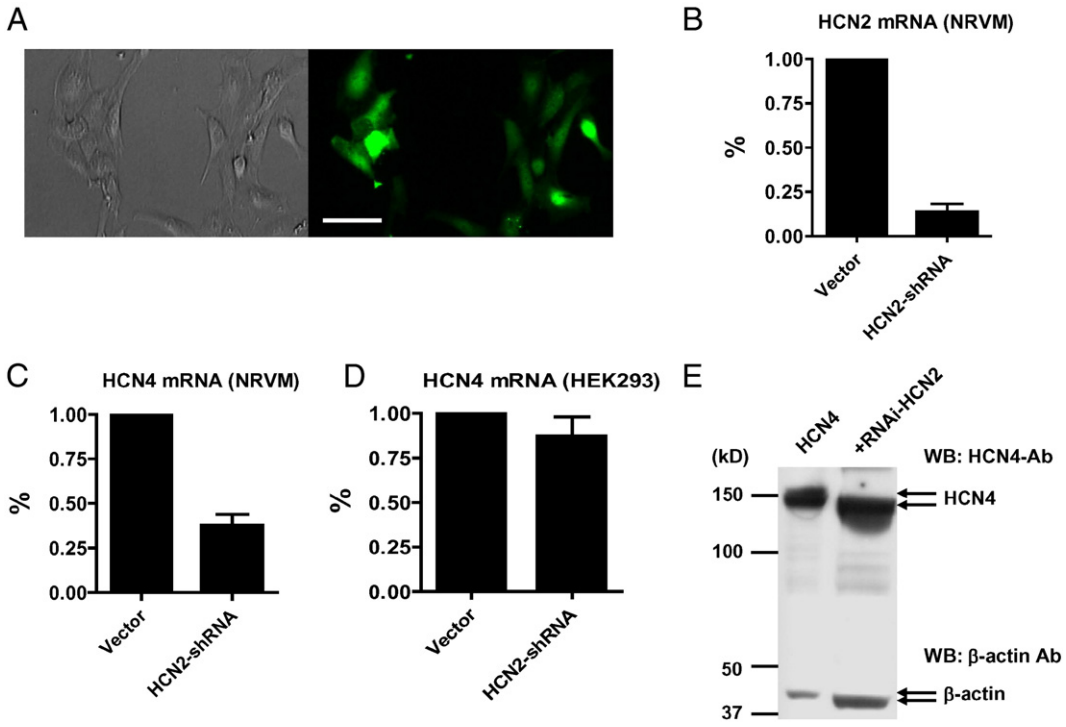

Fig. 5. Association of reduced HCN2 and HCN4 mRNA in neonatal rat ventricular myocytes and controls in HEK293 cells. Neonatal rat ventricular cardiomyocytes were infected by GFP-tagged lentivirus containing shRNA specifically targeted to HCN2. (A) Bright-field (left panel) and fluorescent (right panel) images of NRCM. Scale bar = 10 μm. (B) Reduced HCN2 mRNA by RNAi. (C) Reduced HCN4 mRNA by HCN2 RNAi. Empty vector infection did not significantly affect the HCN2 or HCN4 mRNA. (D) HCN2-shRNA did not affect mRNA of HCN4 expressed in HEK293 cells. HCN4 mRNA was then measured by RT-PCR after 24 h transfection in cells with and without transduction of lentivirus containing HCN2-shRNA. (E) HCN2-shRNA did not affect protein expression of HCN4 expressed in HEK293 cells.

in I_f current density between the non-infected and vector-infected myocytes. Lentivirus infection of myocytes did not cause significant morphological change in myocytes.

Accompanying the increased current amplitude was a positive shift in I_f threshold activation which was −80 mV (arrow) (Fig. 8B). The non-infected myocyte (Fig. 8A) or vector infected myocyte (Fig. 8C) shows I_f with threshold activation around −100 mV (arrow), consistent with our previous reports [16,29]. Averaging over 5–10 myocytes for each group, the threshold for I_f activation was -107 ± 8 mV ($n = 10$) for non-infected myocytes, -76 ± 9 mV ($n = 8$) for HCN4-infected myocytes, and -110 ± 7 mV ($n = 5$) for vector infected myocytes.

In addition, I_f kinetics was also accelerated in HCN4-infected myocytes. At −120 mV or −125 mV, the time constants of current activation were 1.47 ± 0.48 s ($n = 10$) for control and 0.47 ± 0.18 s ($n = 8$) for HCN4-infected myocytes, and 1.69 ± 0.52 s ($n = 5$) for vector-infected myocytes.

4. Discussion

Using a combination of electrophysiology and biochemistry as well as fluorescent imaging techniques, formation of functional heteromeric HCN channels has been investigated for HCN1/HCN2 [5–8], HCN1/HCN4 [9], HCN2/HCN4 [10,11]. Evidence also showed that HCN2 and HCN3 do not associate with each other when they were expressed in HEK293 cells [10].

In this study we presented evidence showing the different properties of HCN2/HCN4 channels expressed in *Xenopus* oocytes from their respective homomeric channels — some of them were unexpected. When HCN2 and HCN4 were expressed in *Xenopus*

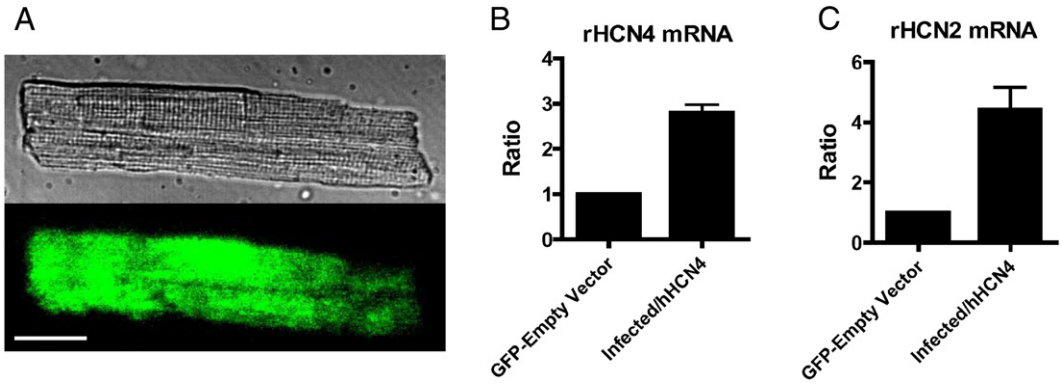

Fig. 6. Association of increased HCN2 and HCN4 mRNA in adult rat myocytes. (A) Bright-field image (upper panel) and fluorescent image (lower panel) of an adult rat ventricular myocyte infected by GFP-tagged lentivirus containing HCN4. Scale bar = 20 μm. (B) Increased HCN4 mRNA in myocytes overexpressing HCN4. (C) Increased HCN2 mRNA in myocytes overexpressing HCN4. Empty virus infection did not significantly affect the HCN2 or HCN4 mRNA, shown as Control.

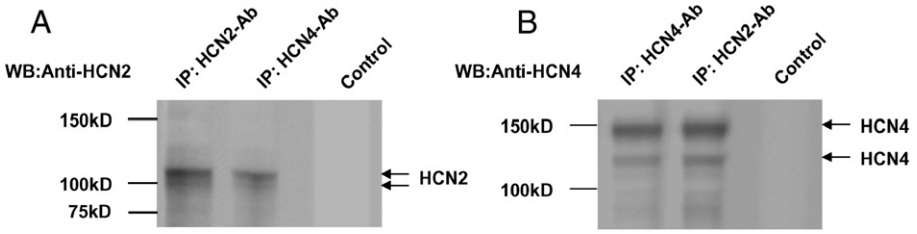

Fig. 7. Association of HCN2 and HCN4 in adult rat ventricles. (A) HCN2 signal detection in samples immunoprecipitated using a HCN4 antibody. HCN2 signal detection in samples immunoprecipitated using the same HCN2 antibody was used as a positive control. (B) HCN4 signal detection in samples immunoprecipitated using a HCN2 antibody. HCN4 signal detection in samples immunoprecipitated using the same HCN4 antibody was used as a positive control. HEK293 cells with no transfection of HCN2 and/or HCN4 were used as negative controls for (A) and (B), respectively.

oocytes separately as homomeric channels, HCN2 showed less negative threshold activation and faster activation kinetics in comparison to HCN4 [14,26]. We therefore anticipated only three outcomes if HCN2 and HCN4 channels gate independently when expressed in oocytes: (1) mixing mRNAs of HCN2 and HCN4 equally (1:1) would generate the channels having intermediate properties — current activation more negative than HCN2 but more positive than HCN4 with activation kinetics slower than HCN2 but faster than HCN4; (2) mixing more HCN2 mRNA with HCN4 (10:1) would generate the channels with gating properties very close to that of HCN2; (3) mixing more HCN4 mRNA with HCN2 (1:10) would generate the channels gating properties very close to HCN4. However, our data showed that all ratios of HCN2 and HCN4 mRNAs resulted in the activation at more depolarized potentials with generally faster activation. The fastest activation was observed surprisingly in channels with a ratio of 0.1, which was predicted to be very close to activation of HCN4 homomeric channels. These results suggested the functional formation of HCN2/HCN4 heteromeric channels which are not simple summation of their respective homomeric channels. They are indicative of the likely results of different modulation of the heteromeric channels as compared to that for homomeric channels. Interestingly, previous studies of HCN1/HCN2 in *Xenopus* oocytes showed intermediate properties which also led to the conclusion of heteromeric channels [5,6].

Discrepancy in midpoint voltages of HCN2 and HCN4 expressed mammalian cells existed in previous reports. Some reported a more depolarized V0.5 for HCN2 than for HCN4 [21–23], while others showed a more hyperpolarized $V_{1/2}$ for HCN2 than for HCN4 [19,20]. This can be caused by many factors such as temperature (room versus body temperature), expression vector, passages of cells, and endogenous proteins that may modulate the properties of HCN channels. Under our experimental conditions, we observed a more depolarized $V_{1/2}$ for HCN2 than for HCN4. The difference, however, is less significant in comparison to the $V_{1/2}$ for HCN2 and HCN4 expressed in *Xenopus* oocytes.

To extend our studies to cardiomyocytes, we explored an idea whether the interaction of HCN2 and HCN4 in myocytes might occur even before the channel proteins are synthesized. We used lentivirus as an effective delivery system, shown in the recent studies for selectively manipulation of ion channel expression in cardiomyocytes (e.g., see ref. [32]), to either down-regulate HCN2 mRNA in neonatal rat ventricular myocytes by an shRNA-directed approach or up-regulate HCN4 mRNA by overexpressing HCN4 in adult rat ventricular myocytes. The reason for altering the HCN mRNA in rat at different ages is that HCN2 and HCN4 expression levels are relatively higher in neonatal and lower in adult rat ventricles [13]. It would be more feasible to inhibit the high mRNA expression in neonatal ventricles and enhance the low mRNA expression in adult ventricles. Although

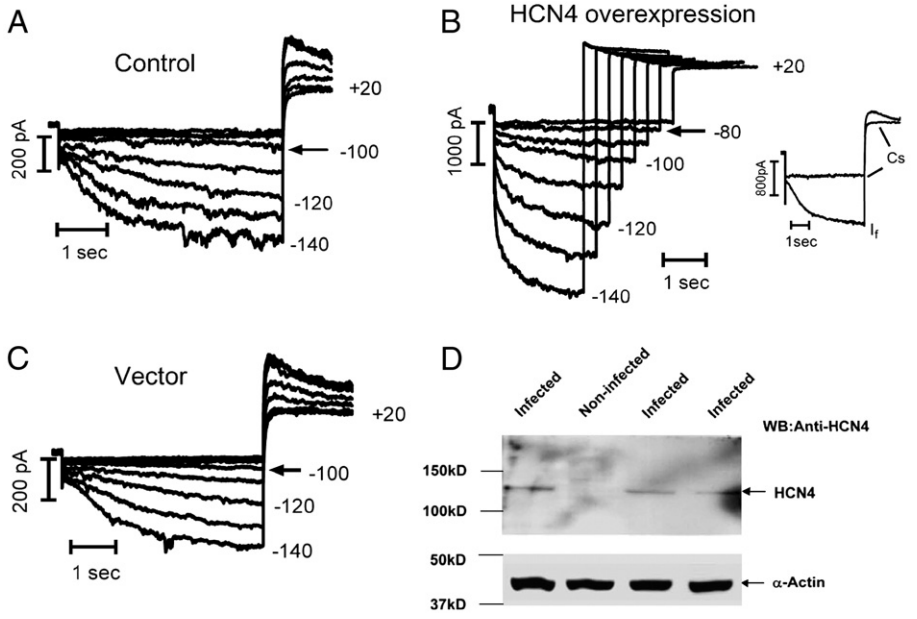

Fig. 8. I_f in adult rat ventricular myocytes without (A) or with empty lentiviral vector infection (C) and with HCN4 overexpression (B) (inset: 4 mM Cs blockade of I_f recorded at −120 mV, 4.5 s pulse duration). The holding potential was −50 mV. Hyperpolarizing pulses for 4.5 s (A, C) or variable durations (B) ranged from −70 mV to −140 mV in 10 mV increments. The tail currents were recorded at +20 mV. (D) Western blot analysis of HCN4 expression in adult rat ventricular myocytes overexpressing HCN4 repeated in three separate samples. Non-infected myocytes were used as a negative control. α-actins were used as loading controls.

much expected, it was still surprising to observe that the targeted HCN2 knockdown was associated with a significant decrease in HCN4 mRNA. Likewise, enhancing the mRNA of HCN4 by overexpression was linked to a dramatic increase in HCN2 mRNA. Moreover, if we increase the ratio of HCN2 and HCN4 mRNA by overexpressing HCN4 in myocytes, we observed enhanced I_f activity that mimics that in neonatal rat ventricular myocytes, a result similar to that we observed in *Xenopus* oocytes. Finally, we confirmed association of HCN2 and HCN4 channels in rat adult ventricles using co-immunoprecipitation experiments.

As it is always the case with unexpected observations, new questions are raised as the underlying mechanisms for the associated alteration of HCN2 and HCN4 mRNAs. The transcript levels are controlled by the promoter activity. There are high sequence similarity in HCN2 and HCN4 promoters [33]. From a speculative viewpoint (since very little is known about gene regulation for HCN channels), there might exist a feedback link between the mRNA synthesis and the promoter activity for HCN channel expression (e.g., [34]). Thus, changes in expression of one isoform can affect the expression of the other. This speculation is partially supported by the data showing that in HEK293 cells (no endogenous HCN channels) HCN2-shRNA did not affect HCN4 mRNA levels (Fig. 4D). In myocytes (both neonatal and adult) where there are significant expression of HCN2 and HCN4, HCN2-shRNA did decrease HCN4 mRNA, but to a lesser degree (Fig. 4D) as compared with HCN2 inhibition (Fig. 4C).

It is worth noting that the voltage-gated potassium channel, Kv1.5, can produce homomeric channels at low concentration and heteromeric channels (with Kv1.4) at high concentration [35]. The ratio of HCN2 over HCN4 mRNA in ventricles changes during development [13]. Thus, the relative abundance of HCN2 and HCN4 might be important in contributing to the assembly of HCN2/HCN4 heteromeric channels in different tissues. If true, the conditions under which the HCN2 and HCN4 can form the heteromeric channels *in vivo* are not only significant in understanding of tissue-specific properties of I_f, but also important in the novel therapeutic development of biological pacemaker (e.g., see [36]). In addition, different levels of HCN2 and HCN4 transcripts provide an additional mechanism that heteromeric channels can be formed with different stoichiometry. Having both homomeric and heteromeric channels may have a unique advantage in the modulation of the expressed current in response to various environmental demands.

A recent report on microRNA inhibition of HCN has shown that the cardiac muscle-specific miR-1 can suppress both HCN2 and HCN4 mRNA [37]. It may provide future direction in the mechanistic study of associated changes in HCN2 and HCN4 mRNA. Due to the non-specific feature of miR-1 which targeted the 3′ untranslated regions of both HCN2 and HCN4, it remains a possibility that when one isoform of HCN is altered, it changes the expression level of miR-1, which in turn, affects the expression level of the other isoforms of HCN.

Part of the results was previously published in an abstract form in Experimental Biology 2007 [30].

Grants

The work was supported by Scientist Development Award of the American Heart Association and National Institutes of Health (HL-075023) and an Institutional Grant to HGY.

Acknowledgements

The initial full length cDNA clones of mouse HCN2 and human HCN4 were generous gifts from Drs. Bina Santoro/Steve Siegelbaum (Columbia University) and UB Kaupp (Institut für Neurowissenschaften und Biophysik 1 Forschungszentrum Jülich). We thank Dr. Chenhong Li for technical assistance in patch clamp recordings of I_{HCN2} during the initial screen of effective shRNA/HCN2 in HEK293 cells.

References

[1] R.B. Robinson, S.A. Siegelbaum, Hyperpolarization-activated cation currents: from molecules to physiological function, Annu. Rev. Physiol. 65 (2003) 453–480.
[2] R. Gauss, R. Seifert, U.B. Kaupp, Molecular identification of a hyperpolarization-activated channel in sea urchin sperm, Nature 393 (1998) 583–587.
[3] A. Ludwig, X. Zong, M. Jeglitsch, F. Hofmann, M. Biel, A family of hyperpolarization-activated mammalian cation channels, Nature 393 (1998) 587–591.
[4] B. Santoro, D.T. Liu, H. Yao, D. Bartsch, E.R. Kandel, S.A. Siegelbaum, G.R. Tibbs, Identification of a gene encoding a hyperpolarization-activated pacemaker channel of brain, Cell 93 (1998) 717–729.
[5] C. Ulens, J. Tytgat, Functional heteromerization of HCN1 and HCN2 pacemaker channels, J. Biol. Chem. 276 (2001) 6069–6072.
[6] S. Chen, J. Wang, S.A. Siegelbaum, Properties of hyperpolarization-activated pacemaker current defined by coassembly of HCN1 and HCN2 subunits and basal modulation by cyclic nucleotide, J. Gen. Physiol. 117 (2001) 491–504.
[7] C. Proenza, N. Tran, D. Angoli, K. Zahynacz, P. Balcar, E.A. Accili, Different roles for the cyclic nucleotide binding domain and amino terminus in assembly and expression of hyperpolarization-activated, cyclic nucleotide-gated channels, J. Biol. Chem. 277 (2002) 29634–29642.
[8] T. Xue, E. Marban, R.A. Li, Dominant-negative suppression of HCN1- and HCN2-encoded pacemaker currents by an engineered HCN1 construct: insights into structure-function relationships and multimerization, Circ. Res. 90 (2002) 1267–1273.
[9] C. Altomare, B. Terragni, C. Brioschi, R. Milanesi, C. Pagliuca, C. Viscomi, A. Moroni, M. Baruscotti, D. DiFrancesco, Heteromeric HCN1–HCN4 channels: a comparison with native pacemaker channels from the rabbit sinoatrial node, J. Physiol. 549 (2003) 347–359.
[10] B. Much, C. Wahl-Schott, X. Zong, A. Schneider, L. Baumann, S. Moosmang, A. Ludwig, M. Biel, Role of subunit heteromerization and N-linked glycosylation in the formation of functional hyperpolarization-activated cyclic nucleotide-gated channels, J. Biol. Chem. 278 (2003) 43781–43786.
[11] G.M. Whitaker, D. Angoli, H. Nazzari, R. Shigemoto, E.A. Accili, HCN2 and HCN4 isoforms self-assemble and co-assemble with equal preference to form functional pacemaker channels, J. Biol. Chem. 282 (2007) 22900–22909.
[12] A. Bartuti, D. DiFrancesco, Control of cardiac rate by "funny" channels in health and disease, Ann. N.Y. Acad. Sci. 1123 (2008) 213–223.
[13] W. Shi, R. Wymore, H. Yu, J. Wu, R.T. Wymore, Z. Pan, R.B. Robinson, J.E. Dixon, D. McKinnon, I.S. Cohen, Distribution and prevalence of hyperpolarization-activated cation channel (HCN) mRNA expression in cardiac tissues, Circ. Res. 85 (1999) e1–e6.
[14] H. Yu, J. Wu, I. Potapova, R.T. Wymore, B. Holmes, J. Zuckerman, Z. Pan, H. Wang, W. Shi, R.B. Robinson, M.R. El-Maghrabi, W. Benjamin, J. Dixon, D. McKinnon, I.S. Cohen, R. Wymore, MinK-related peptide 1: a beta subunit for the HCN ion channel subunit family enhances expression and speeds activation, Circ. Res. 88 (2001) E84–87.
[15] S.S. Arinsburg, I.S. Cohen, H.G. Yu, Constitutively active Src tyrosine kinase changes gating of HCN4 channels through direct binding to the channel proteins, J. Cardiovasc. Pharmacol. 47 (2006) 578–586.
[16] X. Yu, X.W. Chen, P. Zhou, L. Yao, T. Liu, B. Zhang, Y. Li, H. Zheng, L.H. Zheng, C.X. Zhang, I. Bruce, J.B. Ge, S.Q. Wang, Z.A. Hu, H.G.c.-C.A. Yu, Z. Zhou, Calcium influx through If channels in rat ventricular myocytes, Am. J. Physiol. Cell Physiol. 292 (2007) C1147–1155.
[17] Y.H. Lau, R.B. Robinson, M.R. Rosen, J.P. Bilezikian, Subclassification of beta-adrenergic receptors in cultured rat cardiac myoblasts and fibroblasts, Circ. Res. 47 (1980) 41–48.
[18] M.W. Pfaffl, A new mathematical model for relative quantification in real-time RT-PCR, Nucleic Acids Res. 29 (2001) e45.
[19] R. Seifert, A. Scholten, R. Gauss, A. Mincheva, P. Lichter, U.B. Kaupp, Molecular characterization of a slowly gating human hyperpolarization-activated channel predominantly expressed in thalamus, heart, and testis, Proc. Natl. Acad. Sci. U. S. A. 96 (1999) 9391–9396.
[20] T.M. Ishii, M. Takano, L.H. Xie, A. Noma, H. Ohmori, Molecular characterization of the hyperpolarization-activated cation channel in rabbit heart sinoatrial node, J. Biol. Chem. 274 (1999) 12835–12839.
[21] A. Ludwig, X. Zong, J. Stieber, R. Hullin, F. Hofmann, M. Biel, Two pacemaker channels from human heart with profoundly different activation kinetics, EMBO. J. 18 (1999) 2323–2329.
[22] A. Barbuti, B. Gravante, M. Riolfo, R. Milanesi, B. Terragni, D. DiFrancesco, Localization of pacemaker channels in lipid rafts regulates channel kinetics, Circ. Res. 94 (2004) 1325–1331.
[23] A. Moroni, A. Barbuti, C. Altomare, C. Viscomi, J. Morgan, M. Baruscotti, D. DiFrancesco, Kinetic and ionic properties of the human HCN2 pacemaker channel, Pflugers Arch. 439 (2000) 618–626.
[24] C.H. Li, Q. Zhang, B. Teng, S.J. Mustafa, J.Y. Huang, H.G. Yu, Src tyrosine kinase alters gating of hyperpolarization-activated HCN4 pacemaker channel through Tyr531, Am. J. Physiol. Cell Physiol. 294 (2008) C355–362.
[25] J. Huang, A. Huang, Q. Zhang, Y.C. Lin, H.G. Yu, Novel mechanism for suppression of hyperpolarization-activated cyclic nucleotide-gated pacemaker channels by receptor-like tyrosine phosphatase-{alpha}, J. Biol. Chem. 283 (2008) 29912–29919.

[26] H.G. Yu, Z. Lu, Z. Pan, I.S. Cohen, Tyrosine kinase inhibition differentially regulates heterologously expressed HCN channels, Pflugers Arch. 447 (2004) 392–400.
[27] K.J. Fogle, A.K. Lyashchenko, H.K. Turbendian, G.R. Tibbs, HCN pacemaker channel activation is controlled by acidic lipids downstream of diacylglycerol kinase and phospholipase A2, J. Neurosci. 27 (2007) 2802–2814.
[28] P. Pian, A. Bucchi, R.B. Robinson, S.A. Siegelbaum, Regulation of gating and rundown of HCN hyperpolarization-activated channels by exogenous and endogenous PIP2, J. Gen. Physiol. 128 (2006) 593–604.
[29] R.B. Robinson, H. Yu, F. Chang, I.S. Cohen, Developmental change in the voltage-dependence of the pacemaker current, if, in rat ventricle cells, Pflugers Arch. 433 (1997) 533–535.
[30] Q. Zhang, C. Li, H.-G. Yu, RNAi of HCN pacemaker channels in HEK293 cells, Biophys. J. 94 (2008) 2173.
[31] Q. Zhang, H.-G. Yu, Interaction of HCN2 and HCN4 pacemaker channels, 2007 Exp. Biol, Washington DC, 2007, p. 604.611.
[32] E. Cingolani, G.A. Ramirez Correa, E. Kizana, M. Murata, H.C. Cho, E. Marban, Gene therapy to inhibit the calcium channel beta subunit: physiological consequences and pathophysiological effects in models of cardiac hypertrophy, Circ. Res. 101 (2007) 166–175.
[33] X. Luo, H. Lin, Z. Du, J. Xiao, Y. Lu, B. Yang, Z. Wang, Downregulation of microRNA-1/microRNA-133 and overexpression of Sp1 activates re-expression of pacemaker channel genes HCN2 and HCN4 in hypertrophic heart. Circulation 116 (2007) 162.
[34] L. Huo, G. Fu, X. Wang, W.K. Ko, A.O. Wong, Modulation of calmodulin gene expression as a novel mechanism for growth hormone feedback control by insulin-like growth factor in grass carp pituitary cells, Endocrinology 146 (2005) 3821–3835.
[35] E.S. Levitan, K. Takimoto, Dynamic regulation of K+ channel gene expression in differentiated cells, J. Neurobiol. 37 (1998) 60–68.
[36] I.S. Cohen, P.R. Brink, R.B. Robinson, M.R. Rosen, The why, what, how and when of biological pacemakers, Nat. Clin. Pract. Cardiovasc. Med. 2 (2005) 374–375.
[37] J. Xiao, B. Yang, H. Lin, Y. Lu, X. Luo, Z. Wang, Novel approaches for gene-specific interference via manipulating actions of microRNAs: examination on the pacemaker channel genes HCN2 and HCN4, J. Cell Physiol. 212 (2007) 285–292.